

Topologically localized insulators

Bastien Lapierre, Titus Neupert, Luka Trifunovic¹

¹*Department of Physics, University of Zurich, Winterthurerstrasse 190, 8057 Zurich, Switzerland*
(Dated: January 4, 2022)

We show that fully localized, three-dimensional, time-reversal-symmetry-broken Anderson insulators support topologically distinct phases that can be labelled by integers. Any two such topologically localized phases are separated by a metallic phase. We find that these novel topological phases are fundamentally distinct from insulators without disorder: they are guaranteed to host delocalized states along their insulating boundaries, giving rise to the quantized boundary Hall conductance whose value is determined by the integer invariant assigned to the bulk.

Introduction — One of the biggest successes of the Bloch band theory [1] of crystals lies in its ability to explain and predict why some crystals are insulating while others conduct charge current. This theory predicts that insulators have a gap in their band structure, below which all the states are occupied with electrons and are therefore electrically “inert” at zero temperature and as far as bulk properties are concerned. The developments of the last 40 years showed that insulators can exhibit intriguing physics, rooted in their topological properties [2–5]. Such topological (band) insulators (TIs), although insulating in the bulk, have boundaries that are perfect metals [6, 7]. In fact, the phenomenology of the boundary states of TIs is so rich that it allows for situations where only some parts of the boundary are perfect metals while the rest is insulating. These are so-called higher-order TIs [8–11].

Not all insulating crystals are band insulators. In particular, insulators can be Mott insulators [12], where the insulating behavior is explained by electron-electron interactions rather than the existence of the band gap, or Anderson insulators [13], where the insulating behavior is explained by localization of the bulk states by disorder. Under addition of symmetry-persevering disorder, the phase of a trivial band insulator shrinks while neighboring non-trivial (strong) phase expands [14]. Hence, it is possible to start from a trivial band insulator and drive it by disorder into a topologically non-trivial phase called “topological Anderson insulator” [15–17]. Despite this terminology, the topological Anderson insulator and the corresponding topological band insulator belong to the same insulating topological phase.

In this work, we show that fully localized Anderson insulators can be divided into topological equivalence classes. To this end, we consider three-dimensional crystals without time-reversal symmetry (class A), where all strong band insulators are topologically trivial [2, 7]. Our main result is the discovery of topologically distinct, fully localized insulators that can be labeled by integers N_{TLI} , where insulators labeled by different integers are separated by a metallic phase. We dub such topologically non-trivial three-dimensional Anderson insulators *topologically localized insulators* (TLIs). We find that, al-

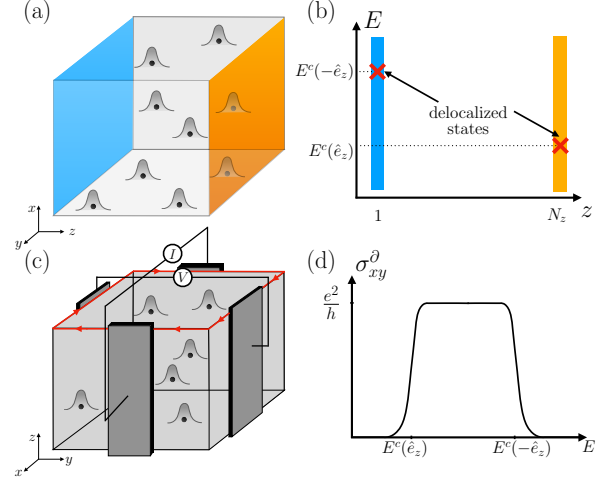


FIG. 1. (a) TLI with $N_{\text{TLI}} = 1$ for open boundary conditions along z only: all the bulk states are localized by disorder, while the two boundary surfaces (orange and blue) host delocalized states and have opposite quantized Hall conductance. (b) The energies $E^c(\pm\hat{e}_z)$ of delocalized states are not constrained by the bulk. (c) Four terminal Hall-measurement setup. When faces of the system have translational symmetry (on average), the chiral hinge modes (red) appear on the top face for $E^c(\hat{e}_z) < E_F^0 < E^c(\pm\hat{e}_{x,y}) < E^c(-\hat{e}_z)$. (d) A non-zero quantized Hall conductance σ_{xy}^0 of the boundary is obtained when the chiral hinge states are present.

though all the bulk states of a TLI are exponentially localized, there is an obstruction in localizing them all the way down to the atomic limit. Once the boundary surface with normal \hat{n} is introduced, topologically protected delocalized states [18, 19] with energies $E_i^c(\hat{n})$, $i = 1, \dots, N_{\text{TLI}}$, emerge and remain so under arbitrary disorder at the boundary; The boundary of TLI is anomalous since it cannot be realized as a two-dimensional system: a disordered two-dimensional Chern insulator can host delocalized states only up to disorder strengths that do not close its mobility gap.

When all the bulk states are localized, by doping the boundary with electrons, the Fermi energy of the boundary E_F^0 can be varied independently of the bulk Fermi energy E_F . When E_F^0 lies in the energy-window(s) spanned by $E_i^c(\hat{n})$ for different \hat{n} , a quantized Hall conductance is

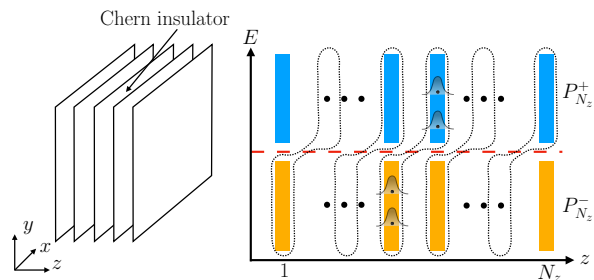


FIG. 2. TLI construction from stack of two-dimensional Chern insulators in z -direction (left panel). The projector onto the Hilbert space defined by the states below (above) the gap (dashed red line) of the layer z is denoted by P_z^+ (P_z^-), shown in blue (orange), has Chern number 1 (-1). After including strong disorder such that the states below the gap of layer z and the states above the gap of layer $z+1$ localize (and trivialize), a TLI phase is obtained (right panel). Layer $z=1$ ($z=N_z$), for open boundary conditions in z -direction, carries Chern number 1 (-1).

obtained, see Fig. 1c,d. Since the bulk does not constrain the energies $E_i^c(\hat{n})$, the bulk topology of TLIs cannot be detected by a four terminal Hall conductance measurement. At the end of this letter, we argue that a TLI in thick Corbino geometry with a fully filled boundary, has a quantized Hall conductance whose value is determined by the bulk.

Model — We introduce a procedure to systematically construct TLI phases with an arbitrary bulk integer invariant N_{TLI} . In the simplest form of this construction, one starts from a stack in z -direction of identical two-dimensional, two-band Chern insulators [20]. We denote by P_z^+ (P_z^- , $z \in \mathbb{Z}$) the projector onto eigenstates with energy below (above) the band gap of a two-dimensional system at layer z , which have the Chern number $\text{Ch} = 1$ ($\text{Ch} = -1$), see Fig. 2. Keeping the layers of Chern insulators decoupled, we include disorder within each layer. Since the Hilbert spaces onto which P_z^\pm projects have non-zero Chern number, they cannot be separately localized. Specifically, the Chern insulator at layer z is localized (and trivialized) only for a strong enough disorder that closes its mobility gap. This way, a trivial TLI is obtained.

If we instead choose to couple layers, and add strong disorder such that the states below the gap of layer z and the states above the gap of layer $z+1$ hybridize and localize (see Fig. 2), a non-trivial TLI is obtained. The non-trivial TLI Hamiltonian can be written as $H = \sum_z H_{z,z+1}$, where

$$H_{z,z+1} = (P_z^- + P_{z+1}^+) H_W (P_z^- + P_{z+1}^+), \quad (1)$$

with $H_W = \sum_{\vec{R},\alpha} W_{\vec{R}\alpha} |g_{\vec{R}\alpha}\rangle \langle g_{\vec{R}\alpha}|$, and $|g_{\vec{R}\alpha}\rangle = |\vec{R}\alpha\rangle + |(\vec{R} + \hat{e}_z)\alpha\rangle$. The orbitals of the above tight-binding model are denoted by $|\vec{R}\alpha\rangle$, with $\alpha \in \{1, 2\}$ an orbital degree of freedom and \vec{R} a three-dimensional lattice vector.

$W_{\vec{R},\alpha}$ are independent, uniformly distributed in $[-W, W]$, random real numbers. The wavefunctions $|w_{\vec{R}\alpha}\rangle = (P_z^- + P_{z+1}^+) |g_{\vec{R}\alpha}\rangle$ are exponentially localized, and orthonormal $\langle w_{\vec{R}'\alpha'} | w_{\vec{R}\alpha}\rangle = \delta_{\vec{R}\vec{R}'} \delta_{\alpha\alpha'}$. The exponential localization of $|w_{\vec{R}\alpha}\rangle$ follows from that of $P_z^\pm |\vec{R}\alpha\rangle$ [21], whereas orthonormality can be satisfied only for the Hilbert space onto which $(P_z^- + P_{z+1}^+)$ projects, see App. C. The states $|w_{\vec{R}\alpha}\rangle$ form the complete set of localized eigenstates of H under periodic boundary conditions (PBC). Although the constructed Hamiltonian H lacks translational symmetry, its eigenstates $|w_{\vec{R}\alpha}\rangle$ are related to each other by translations. Accordingly, the unitary U that diagonalizes H can be written as $U = \bigoplus_{\vec{k}} U_{\vec{k}}$, where \vec{k} is the three-dimensional momentum labeling the irreducible representations of the translation group that generates the lattice with sites \vec{R} . Although not crucial, this property is convenient for analytical computations of the bulk invariant of the above model, see below.

From the above construction of a TLI it is evident that for a z -terminated crystal, the states localized on the surface at $z=1$ (independent of their energy) have the Chern number $n_{\text{TLI}} = \text{Ch} = 1$ while the states on the surface at $z=N_z$ carry the Chern number -1 , see Fig. 1. Additionally, if magnetic flux quantum $\Phi_0 = h/e$ is threaded through the layers, the rank of P_z^- (P_{z+1}^+) decreases (increases) by Ch ($= n_{\text{TLI}}$) according to Streda formula [22]. If the bulk is fully filled with electrons, the applied flux Φ_0 transfers n_{TLI} electrons, from layer z to layer $z+1$, resulting in the bulk polarization $P_z \sim n_{\text{TLI}}$. We conclude that the bulk magnetoelectric polarizability coefficient is quantized, $(\alpha_{\text{ME}})_{zz} = n_{\text{TLI}}$. It is less obvious that the bulk magnetoelectric polarizability tensor is isotropic and that also x - and y -terminated crystals have surfaces with non-zero Chern numbers, which we demonstrate numerically further below.

The described procedure can be easily generalized to a construction of a TLI with an arbitrary surface Chern number n_{TLI} . In the most general form, one starts from the layers with $(m-1)$ band gaps which define Hilbert spaces with Chern numbers Ch_i , with $\sum_{i=1}^m \text{Ch}_i = 0$. By adding disorder we can choose to hybridize and localize states from layer $z=l_1$ with the Chern number Ch_1 , states from layer $z=l_2$ with Ch_2 ..., and the states from layer $z=l_m$ with the Chern number Ch_m . Below we define the bulk integer invariant N_{TLI} that can be computed for an arbitrary fully-localized phase. We find the relation between N_{TLI} and Ch_i to be that of the dipole and charge: $N_{\text{TLI}} = \sum_{i=1}^m l_i \text{Ch}_i$, see App. A. An alternative construction of TLI can be found in App. D.

Bulk integer invariant N_{TLI} — For a localized bulk Hamiltonian H , we define the bulk integer invariant to be the third winding number $\nu[U]$ of a unitary U that diagonalizes H . It is customary to define the third winding number for translationally invariant unitaries [23] $U = \bigoplus_{\vec{k}} U_{\vec{k}}$; Recently, the third winding number [24, 25]

$\nu[U]$ was defined for unitaries U that may lack translational symmetry if they have exponentially localized matrix elements in the atomic basis $|\vec{R}\alpha\rangle$

$$\langle \vec{R}'\alpha' | U | \vec{R}\alpha \rangle \sim e^{-\gamma|\vec{R}-\vec{R}'|}, \quad (2)$$

for some positive constant γ . The condition (2) guarantees that $\nu[U]$ takes integer values [24]. We review definitions of the third-winding number in App. B. For a Hamiltonian with all eigenstates localized, one can define U as mapping eigenstates $|\psi_n\rangle$ of H onto localized orbitals $|\vec{R}\alpha\rangle$, i.e., $U|\vec{R}\alpha\rangle = |\psi_{n(\vec{R},\alpha)}\rangle$, such that condition (2) is satisfied. The assignment defined by $n(\vec{R},\alpha)$ is not unique [26]. We define the bulk integer invariant

$$N_{\text{TLI}} = \langle \nu[U_W] \rangle_W, \quad (3)$$

where we explicitly write dependence of the unitary U on the disorder realization, and $\langle \dots \rangle_W$ is disorder average.

As mentioned above, the construction of the previous section gives a translationally invariant unitary, and one can easily show that for model (1)

$$U_{\vec{k}} = \mathcal{U}_{k_x k_y} \mathcal{D} \mathcal{U}_{k_x k_y}^\dagger, \quad (4)$$

where $\mathcal{U}_{k_x k_y}$ is a unitary that diagonalizes the Bloch Hamiltonian of the two-dimensional, two-band Chern insulator, and the matrix $\mathcal{D} = \text{diag}(e^{ik_z}, 1)$ translates the Bloch eigenstate with the positive energy by one unit cell in z -direction. Using the definition of the third-winding number, it readily follows $N_{\text{TLI}} = 1$, see App. A.

Boundary integer invariant n_{TLI} and bulk-boundary correspondence — We define the boundary integer invariant by considering the slab geometry and selecting the eigenstates of H that are localized on one of the two surfaces $\{|\psi_n^{\text{surf}}\rangle\}$, irrespective of their energy. Since all the bulk states are localized, some of these states can be safely included in the set $\{|\psi_n^{\text{surf}}\rangle\}$; The projector onto these states is denoted by $\mathcal{P}^{\text{surf}} = \sum_n |\psi_n^{\text{surf}}\rangle \langle \psi_n^{\text{surf}}|$. We define the boundary integer invariant as

$$n_{\text{TLI}} = \langle \text{Ch}[\mathcal{P}_W^{\text{surf}}] \rangle_W. \quad (5)$$

Similarly to the third winding number of a unitary, the Chern number [27] can be defined not only for translationally invariant $\mathcal{P}^{\text{surf}} = \bigoplus_{k_x k_y} \mathcal{P}_{k_x k_y}^{\text{surf}}$, but also for $\mathcal{P}^{\text{surf}}$ that lacks translational symmetry if its matrix elements are exponentially localized, analogous to condition (2) with $\mathcal{P}^{\text{surf}}$ in place of U , see App. B.

We are now ready to state the bulk-boundary correspondence of TLI phases

$$N_{\text{TLI}} = n_{\text{TLI}}. \quad (6)$$

We demonstrated that the above relation holds for the model above Eq. (1), for the z -terminated crystal. Below we demonstrate numerically that it also holds for the x -

and y -terminated crystals (hard-wall boundary), as well as for a perturbed version of the model (1). We leave the rigorous proof of relation (6) for the future work, below we give arguments for its validity.

Consider a system described by Hamiltonian H with $N_{\text{TLI}} \neq 0$. Let $H(\lambda)$ continuously interpolate between the system $H(0)$, with PBC in all directions, and $H(1)$, corresponding to the open boundary conditions in z -direction only. We denote the corresponding unitary that diagonalizes $H(\lambda)$ by $U(\lambda)$. Since the slab Hamiltonian $H(1)$ represents a quasi two-dimensional system, it is easy to show that its third winding number has to vanish $\nu[U(1)] = 0$. Since $\nu[U(0)] \neq 0$, we conclude that for some λ the condition (2) has to be violated, i.e., delocalized states appear along the two surfaces of the slab. (This is where the Hamiltonian $H(\lambda)$ is being changed.) Since all other states in the bulk are localized, these delocalized states on the two surfaces can localize only by mutual hybridization. Hence, $N_{\text{TLI}} \neq 0$ implies the existence of surface states that cannot be localized by disorder. This is only possible if they carry a Chern number, which is the statement of relation (6).

The quantized Hall conductance of TLI's boundary comes together with the quantized (isotropic) magnetoelectric polarizability coefficient of its bulk. This follows directly from the arguments presented in Ref. 28: when the slab is fully filled with electrons, the electrons are “inert” and do not respond to an external magnetic field. Since the boundary has non-zero quantized Hall conductance, it follows from the Streda formula that the filling of the boundary changes by an integer amount ($= n_{\text{TLI}}$) when the flux Φ_0 threads the slab. This charge needs to be compensated by the bulk; From this compensation, it follows that the bulk, fully filled with electrons, has quantized magnetoelectric polarizability coefficient $\alpha_{\text{ME}} = n_{\text{TLI}} = N_{\text{TLI}}$.

Numerical results — We perturb the model in Eq. (1) by including nearest-neighbor hopping $H_V(\lambda) = H + \lambda V$ that eventually push the TLI into a metallic phase

$$V = \sum_{\langle \vec{R}\vec{R}' \rangle_\alpha} \left(t_1 |\vec{R}'\alpha\rangle \langle \vec{R}\alpha| + t_2 |\vec{R}'\alpha\rangle \langle \vec{R}\bar{\alpha}| \right) + \text{h.c.}, \quad (7)$$

where $\bar{1} = 2$, $\bar{2} = 1$, and \vec{R} and \vec{R}' are nearest-neighbors. Below, we set $t_1 = 10t_2 = 1$, $W = 1$, and consider one-parameter family of the Hamiltonians $H_V(\lambda)$, $0 \leq \lambda \leq 1$.

We first study the metal-insulator transition using level spacing statistics. To this end, we compute the average level spacing ratio [29, 30] $r = \langle \langle r_n \rangle_n \rangle_W$ around the middle of the spectrum, where $r_n = \min\{s_n, s_{n+1}\} / \max\{s_n, s_{n+1}\}$ with $s_n = E_{n+1} - E_n \geq 0$ being the level spacing. For $\lambda < \lambda_c$ all eigenstates are localized, r decreases with increasing system size, approaching the value $r_{\text{PE}} \approx 0.38$ of the Poisson Ensemble (PE). Note that the last statement is true only for the TLI phase under PBC—under PBC a non-trivial

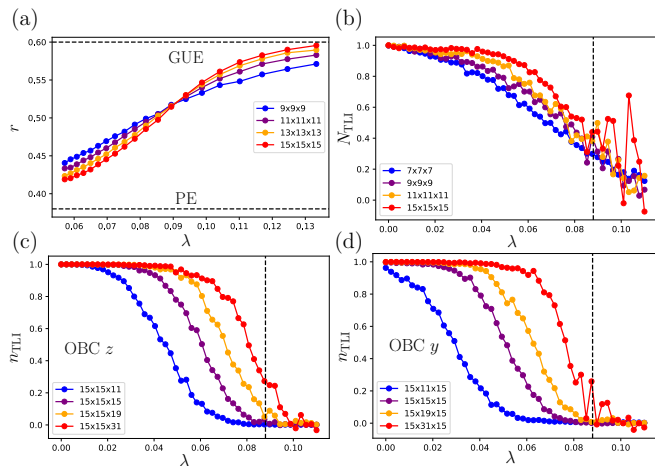


FIG. 3. (a) Estimate of λ_c from mean level spacing ratio r as function of λ . r is computed over 500 eigenstates in the middle of the spectrum, considering 10^3 disorder realizations. (b) The winding number N_{TLLI} is computed for different system sizes with increasing hopping strength λ , where the quantized plateau increases with system size for $\lambda < \lambda_c$. (c) Surface Chern number for the hard-wall termination in z -direction as function of λ . (d) Same as (c), for the termination in y -direction. No disorder averaging was performed for the winding and Chern numbers, apart from the blue curves where average was performed over 5 disorder realizations as well as the red curves in (b) and (c) for $\lambda < \lambda_c$.

TLI phase is unitarily related to a certain trivial TLI phase, hence having the same level spacing statistics. Under open boundary conditions, the non-trivial TLI phase hosts delocalized boundary states and we find that $r \approx 0.43 > r_{\text{PE}}$. For $\lambda > \lambda_c$, the system is in metallic phase at half-filling (mobility edge appears) and r increases with increasing system size, approaching the value $r_{\text{GUE}} \approx 0.60$ of the Gaussian Unitary Ensemble (GUE). From this one-parameter scaling, we find the metal-insulator transition at half-filling occurs at $\lambda_c \approx 0.088 \pm 0.002$, see Fig. 3a.

As long as $H_V(\lambda)$ is in the localized phase, the condition (2) is satisfied and N_{TLLI} and n_{TLLI} are guaranteed to take integer values for large enough system size [24, 27]. In practice, for the system sizes we consider in Fig. 3, we find that the quantization of N_{TLLI} and n_{TLLI} breaks before the value of λ_c is reached. In Fig. 3, we show that the range of λ for which N_{TLLI} and n_{TLLI} are quantized extends as the system size is increased, showing the tendency towards the value λ_c .

Quantized response — As mentioned previously, chiral hinge states that appear in TLIs (see Fig. 1b) are an extrinsic signature, i.e., these can be removed by gluing Chern insulators on the corresponding faces. Without the chiral states, a non-zero quantized Hall conductance can be measured in genus-one (Corbino) geometry. Below we propose a setup, inspired by the setup of Ref. 31, that shows unique quantized signature of the bulk topol-

ogy of TLIs.

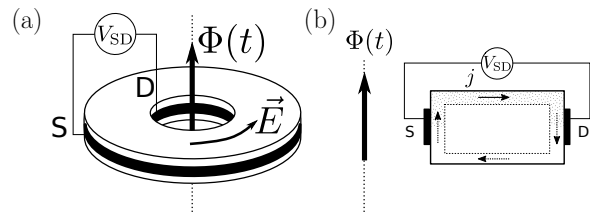


FIG. 4. (a) A non-trivial TLI in Corbino geometry is threaded by magnetic flux $\Phi(t) = \Phi_0 t/T$, with a large source-drain voltage V_{SD} applied. (b) The cross section of the Corbino setup. As the magnetic flux is varied, the charge $e n_{\text{TLLI}}$ is being pumped via the top surface (Laughlin pump). The dotted region (top surface) is filled with electrons in the steady-state, while the bulk is assumed to be empty.

We consider the geometry of a thick Corbino disc, as shown in Fig. 4a, and assume that the boundary is doped with electrons, such that *all* boundary states are occupied. In this setup, an extrinsic second-order TI [32], which consists of a trivial fully-localized bulk with a Chern insulator covering (fully or partially) its boundary, does not react to (adiabatic) time-dependent magnetic flux insertion $\Phi(t) = \Phi_0 t/T$. On the other hand, according to Laughlin argument, the boundary of TLIs pumps n_{TLLI} electrons during the period T around its cross-section, see Fig. 4b. In order to measure this charge pumping, a source-drain voltage, much larger than the bulk mobility gap, is applied. In the presence of such voltage, the charge is removed from the bottom surface. Hence, we expect that in the steady state the top surface remains fully occupied, while the bottom one is empty, see Fig. 4b. (We neglect the effects of the charging energy.) Although such a non-uniform E_F^0 gives rise to chiral states, these states do not connect source to drain: the quantized transfer of n_{TLLI} electrons during one period T occurs via pumping of the boundary states from source to drain via the top surface. Alternatively, by optically exciting [33] the boundary of the system, one could possibly tell TLIs and extrinsic TIs apart.

Conclusions — Topology of TIs [2, 3, 7] poses an obstruction to localization by disorder of its occupied bulk states [18, 19, 34, 35]. Our main result is finding that fully-localized insulators can be topologically non-trivial, too. In particular, we construct a three-dimensional model with broken time-reversal symmetry, where topology poses an obstruction to localization of its fully-localized bulk states all the way down to the atomic limit. We find that the three-dimensional Anderson insulator, with broken time-reversal symmetry, does not represent a single phase of matter, but rather contains infinitely many phases that are labeled by integers. Here, the Anderson model of localization, in the absence of mobility edge, corresponds to topologically trivial insulator and is labelled by $N_{\text{TLLI}} = 0$, whereas topologically non-trivial

localized insulators are guaranteed to host states delocalized along the crystal's insulating boundary that give rise to the quantized Hall conductance $\sigma_{xy}^{\partial} = N_{\text{TLL}}e^2/h$ in Corbino geometry. Crucially, these delocalized boundary states remain topologically protected in the presence of an arbitrarily strong boundary disorder. We introduced the method to construct these novel insulators, which is readily generalizable to include additional symmetries (e.g. time-reversal). We hope that this work will motivate experiments where quantized responses are observed in out-of-equilibrium settings.

Acknowledgments — The authors acknowledge stimulating discussions with Ö. M. Aksoy, P. W. Brouwer, A. Furusaki, and C. Mudry. We are thankful to P. W. Brouwer for pointing up similarities between TLLs and extrinsic TIs. BL acknowledges funding from the European Research Council (ERC) under the European Union's Horizon 2020 research and innovation program (ERC-StG-Neupert-757867-PARATOP). LT acknowledges financial support from the FNS/SNF Ambizione Grant No. PZ00P2_179962.

-
- [1] F. Bloch, *Zeitschrift für Physik* **52**, 555 (1929).
- [2] A. Kitaev, *AIP Conference Proceedings* **1134**, 22 (2009).
- [3] A. P. Schnyder, S. Ryu, A. Furusaki, and A. W. W. Ludwig, *AIP Conference Proceedings* **1134**, 10 (2009).
- [4] B. A. Bernevig and S.-C. Zhang, *Phys. Rev. Lett.* **96**, 106802 (2006).
- [5] M. Z. Hasan and C. L. Kane, *Rev. Mod. Phys.* **82**, 3045 (2010).
- [6] S. Ryu, C. Mudry, H. Obuse, and A. Furusaki, *Phys. Rev. Lett.* **99**, 116601 (2007).
- [7] A. P. Schnyder, S. Ryu, A. Furusaki, and A. W. W. Ludwig, *Phys. Rev. B* **78**, 195125 (2008).
- [8] F. Schindler, A. M. Cook, M. G. Vergniory, Z. Wang, S. S. P. Parkin, B. A. Bernevig, and T. Neupert, *Science Advances* **4** (2018), 10.1126/sciadv.aat0346.
- [9] Z. Song, Z. Fang, and C. Fang, *Phys. Rev. Lett.* **119**, 246402 (2017).
- [10] J. Langbehn, Y. Peng, L. Trifunovic, F. von Oppen, and P. W. Brouwer, *Phys. Rev. Lett.* **119**, 246401 (2017).
- [11] L. Trifunovic and P. W. Brouwer, *physica status solidi (b)*, 2000090 (2020).
- [12] N. F. Mott and R. Peierls, *Proceedings of the Physical Society* **49**, 72 (1937).
- [13] P. W. Anderson, *Phys. Rev.* **109**, 1492 (1958).
- [14] B. Sbierski, G. Pohl, E. J. Bergholtz, and P. W. Brouwer, *Phys. Rev. Lett.* **113**, 026602 (2014).
- [15] C. W. Groth, M. Wimmer, A. R. Akhmerov, J. Tworzydło, and C. W. J. Beenakker, *Phys. Rev. Lett.* **103**, 196805 (2009).
- [16] J. Li, R.-L. Chu, J. K. Jain, and S.-Q. Shen, *Phys. Rev. Lett.* **102**, 136806 (2009).
- [17] H.-M. Guo, G. Rosenberg, G. Refael, and M. Franz, *Phys. Rev. Lett.* **105**, 216601 (2010).
- [18] J. T. Chalker and P. D. Coddington, *Journal of Physics C: Solid State Physics* **21**, 2665 (1988).
- [19] J. Wang, B. Lian, and S.-C. Zhang, *Phys. Rev. B* **89**, 085106 (2014).
- [20] F. D. M. Haldane, *Phys. Rev. Lett.* **61**, 2015 (1988).
- [21] T. Thonhauser and D. Vanderbilt, *Phys. Rev. B* **74**, 235111 (2006).
- [22] P. Streda, *Journal of Physics C: Solid State Physics* **15**, L717 (1982).
- [23] S. Ryu, A. P. Schnyder, A. Furusaki, and A. W. W. Ludwig, *New Journal of Physics* **12**, 065010 (2010).
- [24] J. Song and E. Prodan, *Phys. Rev. B* **89**, 224203 (2014).
- [25] J. Song, C. Fine, and E. Prodan, *Phys. Rev. B* **90**, 184201 (2014).
- [26] $U(1)$ gauge freedom and non-uniqueness of $n(\vec{R}, \alpha)$ do not affect the value of the winding number $\nu[U]$.
- [27] E. Prodan, *Journal of Physics A: Mathematical and Theoretical* **44**, 113001 (2011).
- [28] B. Lapierre, T. Neupert, and L. Trifunovic, *Phys. Rev. Research* **3**, 033045 (2021).
- [29] V. Oganesyan and D. A. Huse, *Phys. Rev. B* **75**, 155111 (2007).
- [30] J. Šuntajs, T. Prosen, and L. Vidmar, *Annals of Physics*, 168469 (2021).
- [31] A. Kundu, M. Rudner, E. Berg, and N. H. Lindner, *Phys. Rev. B* **101**, 041403 (2020).
- [32] M. Geier, L. Trifunovic, M. Hoskam, and P. W. Brouwer, *Phys. Rev. B* **97**, 205135 (2018).
- [33] S. A. Sato, P. Tang, M. A. Sentef, U. D. Giovannini, H. Hübener, and A. Rubio, *New Journal of Physics* **21**, 093005 (2019).
- [34] T. Morimoto, A. Furusaki, and C. Mudry, *Phys. Rev. B* **91**, 235111 (2015).
- [35] M. Onoda, Y. Avishai, and N. Nagaosa, *Phys. Rev. Lett.* **98**, 076802 (2007).
- [36] J. E. Moore, Y. Ran, and X.-G. Wen, *Phys. Rev. Lett.* **101**, 186805 (2008).
- [37] A. Alexandradinata, A. Nelson, and A. A. Soluyanov, *Phys. Rev. B* **103**, 045107 (2021).

SUPPLEMENTARY MATERIAL

A. Computation of the winding number for the model of TLI

In this section we show that the winding number for the model introduced in the main text above Eq. (1), is quantized to a non-zero value given by the Chern number of a single layer.

We first prove relation (4) of the main text. The Bloch states with negative energy at layer z , and positive energy at layer $z + 1$ are

$$\begin{cases} |u_{zk_xk_y}^- \rangle = a_{k_xk_y} |z1\rangle + b_{k_xk_y} |z2\rangle, \\ |u_{(z+1)k_xk_y}^+ \rangle = b_{k_xk_y}^* |(z+1)1\rangle - a_{k_xk_y}^* |(z+1)2\rangle, \end{cases} \quad (\text{S1})$$

where we used the notation $\mathcal{U}_{k_xk_y} = \begin{pmatrix} a_{k_xk_y} & b_{k_xk_y}^* \\ b_{k_xk_y} & -a_{k_xk_y}^* \end{pmatrix}$. The two states above are discontinuous over the BZ. We consider linear combination of the two states that is continuous

$$\begin{cases} |\tilde{u}_{k_xk_y}^- \rangle = a_{k_xk_y}^* |u_{zk_xk_y}^- \rangle + b_{k_xk_y} |u_{(z+1)k_xk_y}^+ \rangle, \\ |\tilde{u}_{k_xk_y}^+ \rangle = b_{k_xk_y}^* |u_{zk_xk_y}^- \rangle - a_{k_xk_y} |u_{(z+1)k_xk_y}^+ \rangle. \end{cases} \quad (\text{S2})$$

After performing a Fourier transform in the z -direction, we conclude that the continuous unitary is of the form

$$U_{\vec{k}}^- = \mathcal{U}_{k_xk_y} \mathcal{D} \mathcal{U}_{k_xk_y}^\dagger, \quad (\text{S3})$$

where $\mathcal{D} = \text{diag}(e^{ik_z}, 1)$. In order to compute the third winding of the above unitary, we use Eq. (S15) which gives eight different terms. We can group four of them as

$$2i \text{Tr} \left(\text{diag}(1, 0) \left[\mathcal{U}_{k_xk_y}^\dagger (\partial_{k_x} \mathcal{U}_{k_xk_y}), \mathcal{U}_{k_xk_y}^\dagger (\partial_{k_y} \mathcal{U}_{k_xk_y}) \right] \right) = 2i \left[\mathcal{U}_{k_xk_y}^\dagger (\partial_{k_x} \mathcal{U}_{k_xk_y}), \mathcal{U}_{k_xk_y}^\dagger (\partial_{k_y} \mathcal{U}_{k_xk_y}) \right]_{00}, \quad (\text{S4})$$

additional two terms as

$$ie^{-ik_z} \left((\partial_{k_x} \mathcal{U}_{k_xk_y}^\dagger) \mathcal{U}_{k_xk_y} \mathcal{D} \mathcal{U}_{k_xk_y}^\dagger (\partial_{k_y} \mathcal{U}_{k_xk_y}) - \mathcal{U}_{k_xk_y}^\dagger (\partial_{k_y} \mathcal{U}_{k_xk_y}) \mathcal{D} (\partial_{k_x} \mathcal{U}_{k_xk_y}^\dagger) \mathcal{U}_{k_xk_y} \right)_{00}, \quad (\text{S5})$$

and the two last terms are

$$ie^{ik_z} \left((\partial_{k_x} \mathcal{U}_{k_xk_y}^\dagger) \mathcal{U}_{k_xk_y} \mathcal{D}^* \mathcal{U}_{k_xk_y}^\dagger (\partial_{k_y} \mathcal{U}_{k_xk_y}) - \mathcal{U}_{k_xk_y}^\dagger (\partial_{k_y} \mathcal{U}_{k_xk_y}) \mathcal{D}^* (\partial_{k_x} \mathcal{U}_{k_xk_y}^\dagger) \mathcal{U}_{k_xk_y} \right)_{00}. \quad (\text{S6})$$

The last two terms cancel out after integrating over k_z from 0 to 2π . Hence, we consider only the terms in Eq. (S4). Using the fact that the Chern number for the lower band reads

$$\text{Ch} = \int_{\text{BZ}} \frac{d^2k}{2\pi i} \left(\langle \partial_{k_x} u_{k_x, k_y}^- | \partial_{k_y} | u_{k_x, k_y}^- \rangle - \langle \partial_{k_y} u_{k_x, k_y}^- | \partial_{k_x} | u_{k_x, k_y}^- \rangle \right) \quad (\text{S7})$$

together with $\mathcal{U}_{k_xk_y} |0\rangle = |u_{k_xk_y}^- \rangle$, and $\mathcal{U}_{k_xk_y}^\dagger (\partial_{k_x} \mathcal{U}_{k_xk_y}) \mathcal{U}_{k_xk_y}^\dagger (\partial_{k_y} \mathcal{U}_{k_xk_y}) = -(\partial_{k_x} \mathcal{U}_{k_xk_y}^\dagger) (\partial_{k_y} \mathcal{U}_{k_xk_y})$, we obtain

$$\nu[U_{\vec{k}}^-] = \text{Ch}. \quad (\text{S8})$$

We note that in the case where $\mathcal{D} = \text{diag}(e^{ilk_z}, 1)$ with $l \in \mathbb{Z}$, the obtained relation becomes $\nu[U_{\vec{k}}^-] = l \text{Ch}$.

The calculation for a more general version of the construction, where each layer has multiple gaps defining Hilbert spaces with Chern numbers Ch_i , see main text, follows along similar lines. Here, the unitary from Eq. (S3) is modified to $U_{\vec{k}}^- = \mathcal{U}_{k_xk_y} \mathcal{D} \mathcal{U}_{k_xk_y}^\dagger$, where $\mathcal{D} = \text{diag}(e^{ik_z l_1}, \dots, e^{ik_z l_{m-1}}, 1)$. (We choose the origin for z such that $l_m = 0$.) It is straightforward to show that Eq. (S4) generalizes to

$$2i \text{Tr} \left(\text{diag}(l_1, \dots, l_{m-1}, 0) \left[\mathcal{U}_{k_xk_y}^\dagger (\partial_{k_x} \mathcal{U}_{k_xk_y}), \mathcal{U}_{k_xk_y}^\dagger (\partial_{k_y} \mathcal{U}_{k_xk_y}) \right] \right). \quad (\text{S9})$$

The above term is equal to $\sum_{i=1}^{m-1} l_i \text{Ch}_i$. Below we show that the remaining,

$$i\text{Tr} \left(\mathcal{D}_1 (\partial_{k_x} U_{k_x k_y}^\dagger) \mathcal{U}_{k_x k_y} \mathcal{D}_2 U_{k_x k_y}^\dagger (\partial_{k_y} \mathcal{U}_{k_x k_y}) - \mathcal{D}_1 U_{k_x k_y}^\dagger (\partial_{k_y} \mathcal{U}_{k_x k_y}) \mathcal{D}_2 (\partial_{k_x} U_{k_x k_y}^\dagger) \mathcal{U}_{k_x k_y} \right) \quad (\text{S10})$$

$$i\text{Tr} \left(\mathcal{D}_1^* (\partial_{k_x} U_{k_x k_y}^\dagger) \mathcal{U}_{k_x k_y} \mathcal{D}_2^* U_{k_x k_y}^\dagger (\partial_{k_y} \mathcal{U}_{k_x k_y}) - \mathcal{D}_1^* U_{k_x k_y}^\dagger (\partial_{k_y} \mathcal{U}_{k_x k_y}) \mathcal{D}_2^* (\partial_{k_x} U_{k_x k_y}^\dagger) \mathcal{U}_{k_x k_y} \right) \quad (\text{S11})$$

with $\mathcal{D}_1 = \text{diag}(l_1 e^{-ik_z l_1}, \dots, l_{m-1} e^{-ik_z l_{m-1}}, 0)$ and $\mathcal{D}_2 = \text{diag}(e^{ik_z l_1}, \dots, e^{ik_z l_{m-1}}, 1)$, vanish. In particular, the sum of Eqs. (S10) and (S11) vanishes after integration over k_z . To this end, we write

$$(\mathcal{D}_1 (\partial_{k_x} U_{k_x k_y}^\dagger) \mathcal{U}_{k_x k_y} \mathcal{D}_2)_{ij} = a_{ij} e^{ik_z (l_i - l_j)} l_j, \quad (\text{S12})$$

with $a_{ij} \equiv ((\partial_{k_x} U_{k_x k_y}^\dagger) \mathcal{U}_{k_x k_y})_{ij}$. Additionally, $(\mathcal{D}_1 (\partial_{k_x} U_{k_x k_y}^\dagger) \mathcal{U}_{k_x k_y} \mathcal{D}_2)_{ij} = (\mathcal{D}_2 (\partial_{k_x} U_{k_x k_y}^\dagger) \mathcal{U}_{k_x k_y} \mathcal{D}_1)_{ij}$ for $l_i = l_j$. We rewrite (S10) as

$$\begin{aligned} i\text{Tr} & \left(\mathcal{D}_1 (\partial_{k_x} U_{k_x k_y}^\dagger) \mathcal{U}_{k_x k_y} \mathcal{D}_2 U_{k_x k_y}^\dagger (\partial_{k_y} \mathcal{U}_{k_x k_y}) - \mathcal{D}_1 U_{k_x k_y}^\dagger (\partial_{k_y} \mathcal{U}_{k_x k_y}) \mathcal{D}_2 (\partial_{k_x} U_{k_x k_y}^\dagger) \mathcal{U}_{k_x k_y} \right) \\ & = i\text{Tr} \left(U_{k_x k_y}^\dagger (\partial_{k_y} \mathcal{U}_{k_x k_y}) \left[\mathcal{D}_1 (\partial_{k_x} U_{k_x k_y}^\dagger) \mathcal{U}_{k_x k_y} \mathcal{D}_2 - \mathcal{D}_2 (\partial_{k_x} U_{k_x k_y}^\dagger) \mathcal{U}_{k_x k_y} \mathcal{D}_1 \right] \right). \end{aligned} \quad (\text{S13})$$

The above trace contains only terms of the form $b e^{iak_z}$. Summing up contributions from Eqs. (S10) and (S11), we obtain only terms proportional to $b \cos(ak_z)$, $a \in \mathbb{Z}$, $b \in \mathbb{C}$, that vanish after integration over k_z . From there it follows,

$$\nu[U_{\vec{k}}] = \sum_{i=1}^{m-1} l_i \text{Ch}_i. \quad (\text{S14})$$

B. Third winding and Chern numbers

For translationally invariant unitaries $U = \bigoplus_{\vec{k}} U_{\vec{k}}$, in the thermodynamic limit, the third winding number is defined

$$\nu[U_{\vec{k}}] = \int_{\text{BZ}} \frac{d^3 k}{8\pi^2} \text{Tr} \left(U_{\vec{k}}^\dagger \partial_{k_x} U_{\vec{k}} \left[U_{\vec{k}}^\dagger \partial_{k_y} U_{\vec{k}}, U_{\vec{k}}^\dagger \partial_{k_z} U_{\vec{k}} \right] \right), \quad (\text{S15})$$

while for finite systems, the integral is replaced by a sum over discrete momenta \vec{k} . For unitaries that lack translational symmetry but satisfy condition (2), the third winding number can be defined [24]

$$\nu[U] = \frac{i\pi}{3} \frac{1}{N_x N_y N_z} \epsilon^{ijk} \text{Tr} \left(U^{-1} [\hat{X}_i, U] U^{-1} [\hat{X}_j, U] U^{-1} [\hat{X}_k, U] \right), \quad (\text{S16})$$

where $\hat{X}_i = \sum_{\vec{R}\alpha} R_i |\vec{R}\alpha\rangle \langle \vec{R}\alpha|$ is the position operator in direction i , and summation over repeated indices is assumed. The above expression takes non-zero integer values only in the thermodynamic limit. In order to apply it to finite systems, we approximate the commutators $[X_i, U]$ by $[\hat{X}_i, U]$, i.e., linear combination of unitaries with integer number of flux quanta inserted

$$[\hat{X}_i, U] = \sum_{m=1}^{N_i-1} c_m e^{2\pi i m \hat{X}_i / N_i} U e^{-2\pi i m \hat{X}_i / N_i}. \quad (\text{S17})$$

The choice of coefficients c_m , giving the correct thermodynamic-limit value of $[X_i, U]$, is not unique [24, 27]. In general, these are the coefficients of the discrete Fourier transform of a function $f(x)$ defined on the circle $[-\frac{N_i}{2}, \frac{N_i}{2}]$ that is periodic and equal to $f(x) = x$ for $x < \alpha \lesssim \lfloor \frac{N_i}{2} \rfloor$. In this work, we take c_m to be the Fourier coefficients of the function $f(x) = x$,

$$c_m = \frac{e^{2\pi i m (\lfloor \frac{N_i}{2} \rfloor + 1) / N_i}}{1 - e^{2\pi i m / N_i}}. \quad (\text{S18})$$

Similarly, for a translationally invariant projector $\mathcal{P} = \bigoplus_{k_x k_y} \mathcal{P}_{k_x k_y}$, in the thermodynamic limit, the Chern number of the Hilbert space, onto which this projector projects, is defined [23]

$$\text{Ch}[\mathcal{P}_{k_x k_y}] = i \int_{\text{BZ}} \frac{dk_x dk_y}{2\pi} \text{Tr} \left(\mathcal{P}_{k_x k_y} [\partial_{k_x} \mathcal{P}_{k_x k_y}, \partial_{k_y} \mathcal{P}_{k_x k_y}] \right), \quad (\text{S19})$$

for finite systems, the above integral is replaced by a sum over discrete momenta (k_x, k_y) . When the projector \mathcal{P} lacks translational symmetry, but satisfied the condition

$$\langle \vec{R}' \alpha' | \mathcal{P} | \vec{R} \alpha \rangle \sim e^{-\gamma |\vec{R} - \vec{R}'|}, \quad (\text{S20})$$

for some positive γ , the Chern number in xy plane in the therodynamic limit can be defined [27]

$$\text{Ch}[\mathcal{P}] = \frac{2\pi i}{N_x N_y} \text{Tr} \left(\mathcal{P} \left[[\hat{X}_1, \mathcal{P}], [\hat{X}_2, \mathcal{P}] \right] \right). \quad (\text{S21})$$

For finite systems, the commutator $[\hat{X}_1, \mathcal{P}]$ is approximated by $[\hat{X}_i, P]$, see Eq. (S17).

C. Details on numerical calculations

For the numerical calculations in this work, the Hamiltonian at each layer z , for the model above Eq. (1), reads

$$H_{2D} = \sin(k_x) \sigma_x + \sin(k_y) \sigma_y + (1 - \cos(k_x) - \cos(k_y)) \sigma_z. \quad (\text{S22})$$

As explained in the main text, the eigenstates of the Hamiltonian above Eq. (1), are

$$|w_{\vec{R}\alpha}\rangle = (P_z^- + P_{z+1}^+) (|\vec{R}\alpha\rangle) + |(\vec{R} + \hat{e}_z)\alpha\rangle, \quad (\text{S23})$$

with eigenenergy $W_{\vec{R}\alpha}$. Hence,

$$H = \sum_{\vec{R}\alpha} W_{\vec{R}\alpha} |w_{\vec{R}\alpha}\rangle \langle w_{\vec{R}\alpha}| \quad (\text{S24})$$

In other words, the above Hamiltonian $H = U H_W U^\dagger$ is unitarily related to Hamiltonian H_W of a trivial localized insulator, with the unitary U satisfying the localization condition (2). To show the orthonormality relation $\langle w_{\vec{R}'\alpha'} | w_{\vec{R}\alpha} \rangle = \delta_{\vec{R}\vec{R}'} \delta_{\alpha\alpha'}$, we denote $\vec{R} = (\vec{r}, z)$, with \vec{r} two-dimensional lattice vector, and consider the scalar product

$$\begin{aligned} \langle w_{\vec{r}'z'\alpha'} | w_{\vec{r}z\alpha} \rangle &= (\langle \vec{r}'z'\alpha' | + \langle \vec{r}'(z+1)\alpha' |) (P_z^+ + P_{z+1}^-) (|\vec{r}z\alpha\rangle + |\vec{r}(z+1)\alpha\rangle) \\ &= \langle \vec{r}'z'\alpha' | P_z^+ |\vec{r}z\alpha\rangle + \langle \vec{r}'z'\alpha' | P_z^- |\vec{r}z\alpha\rangle = \delta_{\vec{r}\vec{r}'} \delta_{\alpha\alpha'}, \end{aligned} \quad (\text{S25})$$

where we used that $P_z^+ + P_z^- = \mathbb{I}$ on the subspace of the Hilbert space corresponding to layer z . For $z \neq z'$, it is sufficient to consider $z' = z + 1$,

$$\begin{aligned} \langle w_{\vec{r}(z+1)\alpha} | w_{\vec{r}z\alpha} \rangle &= (\langle \vec{r}(z+1)\alpha | + \langle \vec{r}(z+2)\alpha |) (P_{z+1}^+ + P_{z+2}^-) (P_z^+ + P_{z+1}^-) (|\vec{r}z\alpha\rangle + |\vec{r}(z+1)\alpha\rangle) \\ &= \langle \vec{r}(z+1)\alpha | P_{z+1}^+ P_{z+1}^- |\vec{r}(z+1)\alpha\rangle = 0. \end{aligned} \quad (\text{S26})$$

In the above derivation, we used that $P_{z+1}^+ P_{z+1}^- = 0$.

Below, we explain how the unitary U_W of the perturbed model $H_V(\lambda)$ is constructed

$$H_V(\lambda) = \sum_{\vec{R}\alpha} \left[W_{\vec{R}\alpha} |w_{\vec{R}\alpha}\rangle \langle w_{\vec{R}\alpha}| + \lambda \sum_{i \in \{x, y, z\}} \left(t_1 \left[|\vec{R} + \hat{e}_i, \alpha\rangle \langle \vec{R}, \alpha | + \text{h.c.} \right] + t_2 \left[|\vec{R} + \hat{e}_i, \alpha\rangle \langle \vec{R}, \bar{\alpha} | + \text{h.c.} \right] \right) \right], \quad (\text{S27})$$

where we set $t_1 = 10t_2 = 1$. All $2N_x N_y N_z$ eigenstates $\{|\psi_n\rangle\}$ of $H_V(\lambda)$ are localized for $\lambda < \lambda_c$ in the thermodynamic limit. The unitary U_W is constructed from these localized eigenstates, after sorting them such that U_W maps $|\vec{R}\alpha\rangle$ to the two eigenstates $|\psi_n(\vec{R}, \alpha)\rangle$, localized closest to the orbitals at $|\vec{R}\alpha\rangle$. To this end, we compute

$\arg(\langle \psi_n | e^{2\pi i \hat{X}_j / N_j} | \psi_n \rangle)$, where the operators $e^{2\pi i \hat{X}_j / N_j}$ are compatible with PBC. This way, we obtain the following coordinate vectors on the 3-torus (\mathbb{T}^3)

$$\vec{v}(|\psi_n\rangle) = \left(\frac{N_x}{2\pi} \arg(\langle \psi_n | e^{2\pi i \hat{X} / N_x} | \psi_n \rangle), \frac{N_y}{2\pi} \arg(\langle \psi_n | e^{2\pi i \hat{Y} / N_y} | \psi_n \rangle), \frac{N_z}{2\pi} \arg(\langle \psi_n | e^{2\pi i \hat{Z} / N_z} | \psi_n \rangle) \right)^T, \quad (\text{S28})$$

where we choose the branch cut of $\arg(\xi)$ to be $[0, \infty)$, such that $0 \leq \arg(\xi) < 2\pi$. The sorting procedure is the following: we first minimize the distance between $\vec{v}(|\psi_n\rangle)$ and $\vec{v}(|\vec{R}\alpha\rangle)$ by computing

$$\|\vec{v}(|\vec{R}\alpha\rangle) - \vec{v}(|\psi_n\rangle)\|_{\mathbb{T}^3} = \sqrt{\sum_{i \in \{x, y, z\}} d(R_i, (\vec{v}(|\psi_n\rangle))_i)^2} \quad (\text{S29})$$

where $d(x, y)$ is the following metric on the circle of radius $\frac{N_i}{2\pi}$,

$$d(x, y) = \min\{|x - y|, N_i - |x - y|\}. \quad (\text{S30})$$

To each orbital $|\vec{R}\alpha\rangle$, we associate eigenvector $|\psi_n\rangle$ closest to it according to the metric (S29), unless this eigenvector is already assigned to a different lattice vector, in which case next-closest unassigned eigenvector is used. This defines a unitary U_W , $U_W |\vec{R}\alpha\rangle = |\psi_n(\vec{R}, \alpha)\rangle$, satisfying the localization condition (2). As the metallic phase is approached, the eigenstates $|\psi_n\rangle$ become plane-wave-like, implying that $|\langle \psi_n | e^{2\pi i \hat{X}_j / N_j} | \psi_n \rangle| \rightarrow 0$. Since $\arg(\xi)$ is not well-defined at $\xi = 0$, the above procedure is not well-define in a metallic phase. For finite systems, we compute $\langle \|\vec{v}(|\psi_n\rangle)\|_{\mathbb{T}^3} \rangle_n$, in order to define the region in parameter space in which the winding number is still well-defined. Such region exists for certain values of λ which are smaller than λ_c , see Fig. 5a.

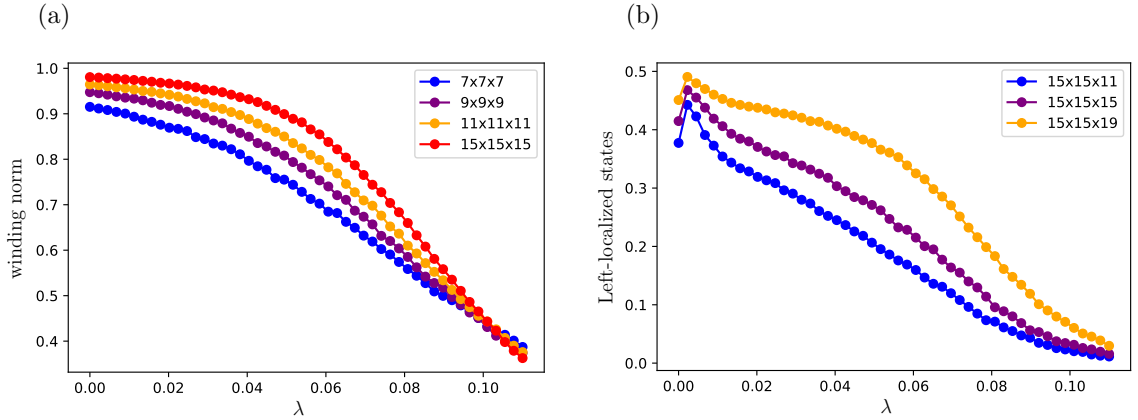


FIG. 5. (a) The average $\langle \|\vec{v}(|\psi_n\rangle)\|_{\mathbb{T}^3} \rangle_n$ over all eigenstates as function of parameter λ , see Eq. (S27). This quantity goes from 1, deep in the localized phase, to 0 in the metallic phase. (b) Portion of eigenstates that are localized in the left-half of the system, i.e. for $z \in \{1, \dots, \lfloor N_z/2 \rfloor\}$. This fraction goes from approximately one-half, at $\lambda = 0$, to 0, for $\lambda > \lambda_c$.

We now define the projector $\mathcal{P}_W^{\text{surf}}$ onto the surface perpendicular to z -axis. This is achieved by removing localized eigenstates $|\psi_n\rangle$ within the bulk of the system, such that the obtained projector projects onto two decoupled surfaces. We first define the set of localized eigenstates in the bulk of the slab as

$$\text{bulk}(W) = \left\{ |\psi_n\rangle, 1 - \sum_{\substack{R_x, R_y, \alpha, \\ R_z = \lfloor N_z/2 \rfloor - L \\ R_z = \lfloor N_z/2 \rfloor + L}} |\langle \vec{R}\alpha | \psi_n \rangle|^2 < \epsilon \right\}, \quad (\text{S31})$$

where L is some bulk cut-off that needs to be large enough such that the upper and lower boundaries are fully decoupled, and ϵ is taken to be 10^{-1} . The eigenstates that do not belong to $\text{bulk}(W)$ are assigned to one of the two boundary surfaces which defines the projector $\mathcal{P}_W^{\text{surf}}$

$$\mathcal{P}_W^{\text{surf}}(\vec{x}, \vec{x}') = \left[\delta_{\vec{x}, \vec{x}'} - \sum_{|\psi_n\rangle \in \text{bulk}(W)} \psi_n(\vec{x}')^* \psi_n(\vec{x}) \right] \theta(z - \lfloor N_z/2 \rfloor) \theta(z' - \lfloor N_z/2 \rfloor), \quad (\text{S32})$$

where $\theta(z)$ is the Heaviside theta function, and we assumed that the plane $z = \lfloor N_z/2 \rfloor$ passes through the middle of the slab. As the system approaches metallic phase, portion of surface-localized states decreases to zero, see Fig. 5b.

D. Relation between TLIs and N -band Hopf insulators

The models of TLIs, introduced in Eq. (1), as well as its N -band generalization discussed in the main text and App. A, become translationally invariant if we change $W_{\vec{R}\alpha}$ from being random numbers to $W_{\vec{R}\alpha} = \alpha$, with $\alpha = 1, \dots, N$. Such deformation of the model does not change the unitary (S3); The resulting, translationally invariant model, corresponds to topologically non-trivial N -band Hopf insulator [28]. Nevertheless, TLIs and N -band Hopf insulators belong to different phases of matter: the constraint of fully-localized bulk implies that TLIs are insulating at an arbitrary filling, whereas N -band Hopf insulators are insulating only at integer fillings. This distinction is important, since it implies that the boundary Fermi energy E_F^0 of N -band Hopf cannot be varied independently of that of the bulk. As a consequence, its quantized boundary response can be measured only in a transient state [28].

Topology of N -band Hopf insulator crucially depends on the presence of translational symmetry. For example, inclusion of perturbations that reduce the translational symmetry down to one of its subgroups can trivialize N -band Hopf insulators [28]. Nevertheless, we show that every N -band Hopf insulator can be deformed to a TLI phase with the same bulk topological invariant. We illustrate this point using $N = 2$ Moore-Ran-Wen model [36]. The two-band Bloch Hamiltonian is defined as

$$h_{k_x k_y k_z} = \vec{v} \cdot \vec{\sigma}, \quad (\text{S33})$$

with $v_i = \vec{z}^\dagger \sigma_i \vec{z}$, where $\vec{z} = (z_1, z_2)^T$, with $z_1 = \sin(k_x) + i \sin(k_y)$ and $z_2 = \sin(k_z) + i[\cos(k_x) + \cos(k_y) + \cos(k_z) - \frac{3}{2}]$. The unitary $U_{\vec{k}}$, that diagonalizes above Bloch Hamiltonian, has a non-zero third winding number $\nu[U_{\vec{k}}] = 1$. The two normalized eigenvectors of the Bloch Hamiltonian (S33) are

$$\begin{aligned} |u_{\vec{k}1}\rangle &= |\vec{z}|^{-1} (z_1, z_2)^T, \\ |u_{\vec{k}2}\rangle &= |\vec{z}|^{-1} (z_2^*, -z_1^*)^T, \end{aligned} \quad (\text{S34})$$

which are continuous functions of \vec{k} . We extend these two Bloch eigenvectors to the whole lattice by defining $\psi_{\vec{k}\alpha}(\vec{x}) = e^{-i\vec{k}\cdot\vec{x}} u_{\vec{k}\alpha}(\vec{x})$. Using these two Bloch eigenvector, we define Wannier functions $|w_{(0,0,0)\alpha}\rangle$, $\alpha = 1, 2$,

$$|w_{\vec{R}\alpha}\rangle = \frac{1}{\sqrt{N_x N_y N_z}} \sum_{\vec{k}} e^{i\vec{k}\cdot\vec{R}} |\psi_{\vec{k}\alpha}\rangle. \quad (\text{S35})$$

We use the above Wannier functions to define the following disordered Hamiltonian

$$H_1 = \sum_{\vec{R}\alpha} W_{\vec{R}\alpha} |w_{\vec{R}\alpha}\rangle \langle w_{\vec{R}\alpha}|. \quad (\text{S36})$$

As the bulk Wannier functions of the Hopf insulator are exponentially localized, the unitary $U|\vec{R}\alpha\rangle = |w_{\vec{R}\alpha}\rangle$ satisfies localization condition (2) and the winding number can be computed using (S16), $\nu[U] = \nu[U_{\vec{k}}] = 1$. By virtue of the bulk-boundary correspondence of the Hopf insulator [28, 37], imposing open boundary conditions in any of the three spatial directions results in surface Chern number equal to $\nu[U] = 1$.